ASCE

Blast Risk Assessment of Wood Residential Buildings: West Fertilizer Plant Explosion Case

Zhenhua Huang, A.M.ASCE[1]; Xun Wang[2]; Liping Cai[3]; Yong Tao[4]; William J. Tolone[5]; Mohammed El-Shambakey[6]; Sreyasee Das Bhattacharjee[7]; and Isaac Cho[8]

Abstract: To predict the hazard-induced risks of buildings and infrastructures and assess the losses caused by hazards, the fragility curve method is a common quantitative risk assessment procedure for civil structures. It has been popularly used for decades for different hazards including earthquakes, hazardous winds, tsunamis, and fires. However, there are limited reports regarding blast risk assessment of buildings using the fragility curve method. This study developed empirical blast fragility curves for wood residential buildings using the real 2013 West fertilizer plant explosion data. The development processes included five key steps: (1) selecting and calculating the blast hazard intensity measure and the air-blast incident overpressure; (2) selecting the damage states rating systems and classifying the damage state of each damaged building; (3) determining the frequency distribution of damaged buildings for each damage state; (4) proving the cumulative lognormal distribution function to describe the fragility relationship between the blast damage states and the blast hazard intensity measure; and (5) constructing the empirical fragility curves by fitting the building damage information to the selected fragility relationship distribution function. The resulted blast fragility curves of this study can be used by government officials to predict blast-induced damages of residential buildings, to plan the optimal locations and operational capacities of emergency facilities, to estimate total economic losses due to potential explosions, and to plan the social, physical and economic resilience of communities. **DOI: 10.1061/(ASCE)CF.1943-5509.0001414.**

[1]Associate Professor, Dept. of Engineering Technology, College of Engineering, Univ. of North Texas, 3940 N. Elm St. F115M, Denton, TX 76207 (corresponding author). ORCID: https://orcid.org/0000-0001-5990-8425. Email: zhenhua.huang@unt.edu

[2]Research Assistant, College of Engineering, Univ. of North Texas, 3940 N. Elm St., Denton, TX 76207. Email: XunWang@my.unt.edu

[3]Research Professor, College of Engineering, Univ. of North Texas, 3940 N. Elm St., Denton, TX 76207. Email: Liping.Cai@unt.edu

[4]Interim Chair & BLG Endowed Professor, Dept. of Mechanical Engineering, Cleveland State Univ., Cleveland, OH 44115. Email: y.tao19@csuohio.edu

[5]Professor, Dept. of Software and Information Systems, College of Computing and Informatics, Univ. of North Carolina at Charlotte, 9201 University City Blvd. 443H, Charlotte, NC 28223. Email: William.Tolone@uncc.edu

[6]Postdoctoral Research Fellow, College of Computing and Informatics, Univ. of North Carolina at Charlotte, 9201 University City Blvd., Charlotte, NC 28223; Researcher, Knowledge-Based and AI Systems, SRTA-City, Universities and Research District, New Borg Elarab, Alexandria 21934, Egypt. ORCID: https://orcid.org/0000-0001-6059-5032. Email: melshamb@uncc.edu; mshambakey@srtacity.sci.eg

[7]Assistant Professor of Teaching, Dept. of Computer Science and Engineering, State University of New York at Buffalo, NY 14260; Adjunct Professor, College of Computing and Informatics, Univ. of North Carolina at Charlotte, Charlotte, NC 28223. Email: sreyasee@buffalo.edu; sdasbhat@uncc.edu

[8]Assistant Professor, Dept. of Computer Science, North Carolina Agricultural and Technical State Univ., 1601 E. Market St., Greensboro, NC 27411; Adjunct Professor, College of Computing and Informatics, Univ. of North Carolina at Charlotte, Charlotte, NC 282231. Email: icho1@uncc.edu; icho@ncat.edu

Note. This manuscript was submitted on February 5, 2019; approved on September 23, 2019; published online on February 29, 2020. Discussion period open until July 29, 2020; separate discussions must be submitted for individual papers. This paper is part of the ***Journal of Performance of Constructed Facilities***, © ASCE, ISSN 0887-3828.

Introduction

In the twenty-first century, the hazard-induced damages of buildings and infrastructures and the hazard-induced losses of life and property are the major challenges for civil engineers and researchers. Quantitative risk assessment is commonly used to predict the hazard-induced risks of buildings and infrastructures and assess the losses caused by the hazards. Fragility curve method is a popular quantitative risk assessment procedure for civil structures under different hazards, such as earthquakes (Calabresea and Lai 2013; Ghosh et al. 2013; Jeong and Elnashai 2007; Khalfan et al. 2016; Lagaros and Fragiadakis 2007; Mai et al. 2017; Mitropoulou and Papadrakakis 2011; Wang et al. 2018; Zentner et al. 2017), hazardous winds (Ataei and Padgett 2015; Herbin and Barbato 2012; Konthesingha et al. 2015; Maloney et al. 2018; Mishra et al. 2017; Stewart et al. 2016), tsunamis (Macabuag et al. 2018; Rehman and Cho 2018), and fires (Gernay et al. 2016). Fragility curve is defined as the relationship between the intensity of a hazard and the probability of a certain response or damage level of civil structures, which indicates the probability of exceeding a damage threshold as a function of a stressor, such as the peak wind gust speed for hurricanes, for a given structure, condition, and damage level. Fragility curves are often associated with probability distributions such as the normal, lognormal, and uniform distributions, in which the most commonly used one is the lognormal distribution (Jeong and Elnashai 2007; Khalfan et al. 2016). Fragility curves are usually categorized into four types based on the damage data used when generating the curves, which are empirical fragility curves, judgmental fragility curves, analytical fragility curves, and hybrid fragility curves. The empirical, judgmental, analytical, and hybrid fragility curves are derived primarily from observed posthazard surveys, expert opinions, analytical simulations, and the combination of these methods, respectively (Rossetto and Elnashai 2003).

The empirical fragility curves are developed according to statistical analyses of observed damages from past hazards, therefore they are the most practical and reliable ones but highly specific to a particular situation and limited for presenting a specific type of building damages (Rossetto and Elnashai 2003). The first fragility curve for quantitative risk assessment for hazards was developed by Veneziano et al. (1983) for earthquake hazards. Since then, the fragility curve method has been used for decades and extended to other hazards including hazardous winds and flooding.

Seismic (earthquake) risk assessment (SRA) using fragility curve method has been widely used to predict the seismic risk of buildings (Calabresea and Lai 2013; Ghosh et al. 2013; Khalfan et al. 2016; Kunnath 2018; Lagaros and Fragiadakis 2007; Lallemant et al. 2015; Mai et al. 2017; Mitropoulou and Papadrakakis 2011; Noh et al. 2015; Shinozuka et al. 2000; Wang et al. 2018; Zentner et al. 2017). The earthquake fragility curves are usually defined as the conditional probabilities of failure of civil structures or critical components according to the values of a seismic intensity measure, such as the peak ground acceleration (PGA) (Khalfan et al. 2016).

Wind (including hurricanes, cyclones, typhoons, and tornados) risk assessment (WRA) of buildings using the fragility curve method usually utilizes fragility curves to express building damages as a function of wind speed (Stewart et al. 2016). Two types of popular wind fragility curves are empirical wind fragility curves developed by curve fitting using the historical wind damage data or loss records, and analytical wind fragility curves developed by modeling the behavior of a building and its components using engineering and structural reliability models (Ataei and Padgett 2015; Herbin and Barbato 2012; Konthesingha et al. 2015; Maloney et al. 2018; Mishra et al. 2017; Stewart et al. 2016). Quantitative risk assessment of buildings using the fragility curve method has been applied to other hazards as well, such as tsunami and fires (Gernay et al. 2016; Macabuag et al. 2018; Rehman and Cho 2018).

The Federal Emergency Management Agency (FEMA 2009, 2011, 2012), an agency of the United States Department of Homeland Security, has adopted the quantitative risk assessment using the fragility curve method in their published analytical tool Hazards United States (HAZUS) (FEMA 2009, 2012) to estimate damages and losses resulted from natural hazards including winds, earthquakes, and floods. HAZUS has been widely used by the government for resilience and sustainability analysis and by insurance companies to estimate insurance payments. For example, the HAZUS Hurricane Model (hurricane loss estimation methodology) uses hurricane fragility curves to estimate potential losses by hurricane hazards. Users anticipate the damages for future hurricanes. Along with the GIS database attached to HAZUS, users can estimate the economic and social losses for any small or large geographic areas for future hurricane hazards. Although the HAZUS Hurricane Model addresses only hurricanes, its application can be extended to other damaging winds such as tornadoes, thunderstorms, extratropical storms, and hailstorms.

Blast is another important hazard that induces significant damages to civil structures especially residential buildings. However, studies regarding civil structures against practical explosion are limited, especially for wood residential buildings, because there is not much available information regarding practical blast hazards and their resulted damages. Stewart and Netherton (2008) carried out the probabilistic risk assessment of glazing subject to explosive blast loading. Abdollahzadeh and Nemati (2014) explored the effects of the direct blast (e.g., a pack portable bomb attacking the city by terrorists) on life losses and injuries, structural collapse, debris impact, fire, and smoke. The blast fragility was estimated by a simulation procedure that generated possible blast configuration, and finally, a kinematic plastic limit analysis was used to verify the structural stability under gravity loading. Fulvio (2015) evaluated the blast fragility of reinforced concrete columns for two classes of European residential buildings based on two different codes, i.e., traditional and earthquake resistant codes. It was concluded that blast fragility surfaces and probabilistic pressure-impulse diagrams could be used for quantitative risk analysis. Faghihmaleki et al. (2017) proposed a probabilistic framework for blast threats in the seismic risk of the RC moment frame with the shear wall structure. The blast fragility was calculated using a Monte Carlo simulation procedure for generating blast scenarios. Yu et al. (2018) generated fragility curves for RC columns by taking the parameter uncertainties in materials, dimensions, and bearded loads into account under blast loads by the deterministic nonlinear analytical approach. The fragility curves were developed using the Monte Carlo simulation. The damages of a typical RC column under blast loads were assessed with the developed fragility curves. These studies are neither about wood residential buildings (the dominant residential building type in the US) nor using empirical data, therefore there is a strong need for an empirical blast fragility analysis for wood residential buildings.

A practical explosion occurred at a fertilizer plant in the town of West, Texas, on April 17, 2013, devastating a populated neighborhood. There have been many studies regarding this practical blast hazard published to date. However, most of the studies focused on the cause of the explosion and government regulations. For example, Yonekawa et al. (2014) analyzed the ocular blast injuries in the West explosion and proposed some safety suggestions, such as staying away from windows during disasters, having first responders use rigid eye shields, and keeping reliable communications. Jennings and Matthiessen (2015) reported that the West explosion triggered efforts by the federal government to improve their coordination with local governments and federal agencies updating policies, regulations, and standards and to pay attention to the safety work practice. Laboureur et al. (2016) identified gaps between the West explosion and the current regulations, then recommended emergency response procedures and provided suggestions for modifying the current regulations to prevent or minimize future losses. Babrauskas (2016, 2017) and Davis et al. (2017) pointed out that untrained fertilizer mill personnel caused this ammonium nitrate (AN) explosions at West, Texas, although several federal and state agencies have made regulations to train personnel in the use of AN. The explosions of the AN fertilizer in storage caused uncontrollable fires. The disaster could be prevented if the potential for the uncontrolled fire was effectively eliminated by implementing fertilizer formulations to reduce uncontrolled fire possibility and adopting building safety measures against uncontrolled fires. Han et al. (2016) indicated that there is a great need to investigate the safer use of AN fertilizers and their alternatives. Han et al. (2017) further discussed the possible physical and chemical reaction between water and AN stock in fires and questioned if the water addition favored the conditions for an explosion, therefore calling for further studies aiming at an optimal procedure for AN fertilizer fires.

However, there are limited studies discussing the structural damages caused by the West explosion. Huang et al. (2016) documented the building damages caused by the West explosion, evaluated the damaged construction and building materials, and calculated the air-blast incident overpressures. Dai et al. (2016) further analyzed the ground shock–induced building damages for the West explosion and calculated ground vibration peak particle velocities (PPVs). It was found that the damages of both wood light-frame buildings and engineered buildings were caused primarily by the air-blast incident overpressure and secondarily by the ground shock.

This study constructed empirical blast fragility curves for wood residential buildings from the real West explosion data.

The proposed empirical blast fragility curve construction procedure can be adopted by researchers for other cases. The developed blast fragility curves in this study can provide structural engineers and researchers with fundamental information for the risk analysis of residential buildings against blast hazards, and provide government agencies with a tool to predict future blast risks.

Blast Hazard Intensity Measure: Air-Blast Incident Overpressure

The air-blast incident overpressure is selected as the blast hazard intensity measure in this study. The air-blast incident overpressure depicts the prompt energy release over the short time period of a blast, which measures the air-blast pressure shockwave moving away from the site of the blast (Baker et al. 1983). The positive overpressure is the difference between the blast pressure and ambient pressure at the given time after blast occurs. The pressure increases instantaneously from ambient pressure due to the explosion, resulting in the maximum positive incident overpressure (Baker et al. 1983).

Several methods are currently available to calculate the air-blast incident overpressure (e.g., Brode 1955; Chang and Young 2010; Held 1983; Henrych 1979; Mills 1987; UFC 2008). Based on the analysis in Huang et al. (2016), two calculation methods, i.e., Held (1983) and UFC (2008), are selected to estimate the air-blast incident overpressure in this study.

Held (1983) proposed that the air-blast incident overpressure, p_s, on the envelope of civil structures can be calculated using a scaling law, which is a function of the dimensional distance parameter (scaled distance) z

$$p_s = \frac{2}{z^2} \tag{1}$$

The calculated p_s is in megapascals. The scaled distance z can be calculated as

$$z = \frac{R}{W^{\frac{1}{3}}} \tag{2}$$

where R = actual effective standoff distance from the explosion center (m); and W = equivalent trinitrotoluene (TNT) mass of the explosive (kg).

Unified Facilities Criteria (UFC) 3-340-02 of Department of Defense (UFC 2008) published a scaling law by using a diagram. The diagram evaluates the positive phase shock wave parameters for a hemispherical TNT explosion, including the air-blast incident overpressure, p_s.

While calculating the air-blast incident overpressure of the damaged wood residential buildings for the West explosion case, the lower bound and upper bound TNT-equivalent mass was assumed to be equal to 6,804 kg (15,000 lbs) and 9,072 kg (20,000 lbs), respectively (Huang et al. 2016). The average value of this upper and lower bound was used as the W in the calculation of this study.

Damage States of Wood Residential Buildings

In addition to the hazard intensity measure discussed in the previous section, the damage state (DS) (different damage levels/scales) is the other important concept for the fragility curve construction. Two damage state rating systems for wood residential buildings were adopted in this study, namely the rating system of HAZUS Hurricane Model for hazardous wind damages versus the rating system of Huang et al. (2016) for blast-induced damages (Table 1).

The rating system of the HAZUS Hurricane Model was developed based on the posthurricane field investigation and the method of finite-element analysis. As shown in Table 1, five damage scales, e.g., no damage (DS0), minor damage (DS1), moderate damage (DS2), severe damage (DS3), and destruction (DS4) were included. For each damage scale, quantitative values of damages on windows, roofs, walls, and structural members were listed to help engineers make a judgment. This rating system was specifically defined for hurricane hazards and can be extended to other hazardous winds. Because of the similarity between wind-induced damages and air-blast–induced damages, this rating system was selected by this study for the blast-induced damage analysis.

The rating system of Huang et al. (2016) was developed based on the practical residential building damage data collected immediately after the West fertilizer plant explosion. A total of 72 damaged wood light-frame buildings were analyzed to develop the rating system, including 65 residential houses, one 2-story apartment complex, one nursing home, one clinic office building, two church buildings, and two storage facilities. As illustrated in Table 1, the severity of the damage to the wood light-frame buildings caused by the West fertilizer plant explosion was classified with four

Table 1. Damage states of Huang et al. (2016) versus HAZUS Hurricane Model (FEMA 2012)

Damage state	Description	Damage description[a]	Damage description[b]
1	Minor damage	Typical window glass breakage; large and small windows shattered; occasional damage to window frames; minor damage to house surfaces	>2% and ≤15% roof cover failure; one window, door, or garage door failure; less than 5 missile impacts on walls
2	Repairable moderate damage	Moderate damage to roof (small deflections, large size, or amount of shingle torn-offs); moderate damage to brick façade (small areas of collapse and cracks) and wall panels (small holes on wood panel, metal panel failure, and buckling)	>15% and ≤ 50% roof cover failure; greater than one and less than or equal to the larger of 20% and three window, door, or garage door failures; 1–3 roof panel failures; typical 5–10 missile impacts on walls
3	Hazardous severe damage	Severe roof surface damage (holes and large deflections), severe wall surface damage (large area of façade collapse and large holes on wood panels), some structural member damage	>50% roof cover failure; greater than the larger of 20% and 3 and ≤50% window, door, or garage door failure; greater than 3 and ≤25% roof panel failures; Typical 10–20 missile impacts on walls
4	Destructive failure	Collapse of roofs and walls, failures of structural members	Typical >50% roof cover failure; >50% window, door, or garage door failure; >25% roof panel failure; typical >20 impacts missile impacts on walls; wall structure failure

[a]Data from Huang et al. (2016).
[b]Data from FEMA (2012).

J. Perform. Constr. Facil., 2020, 34(3): 04020022

damage scales, i.e., minor damage (DS1), repairable moderate damage (DS2), hazardous severe damage (DS3), and destructive failure (DS4). More detailed damage state description can be found in Huang et al. (2016).

Fig. 1 compares Damage states DS1 through DS4 defined in the HAZUS Hurricane Model and Huang et al. (2016). Based on the comparison of damage pictures in Fig. 1 and the damage state descriptions in Table 1, it was obvious that Huang et al. (2016)'s rating system classified more serious damages for almost all damage states. For example, Damage state DS2 (minor damage) in Huang et al. (2016) included a wide variety of glass breakages and minor damages to house surfaces, but it only included one window failure and very tiny missile impacts on walls in the HAZUS Hurricane Model. Similarly, Damage state DS4 (hazardous severe damage) in Huang et al. (2016) includes some structural member damage, but in the HAZUS Hurricane Model it does not.

Geodatabase for West Fertilizer Plant Explosion

The geospatial information (standoff distances from the explosion center) for each building was needed to calculate the air-blast

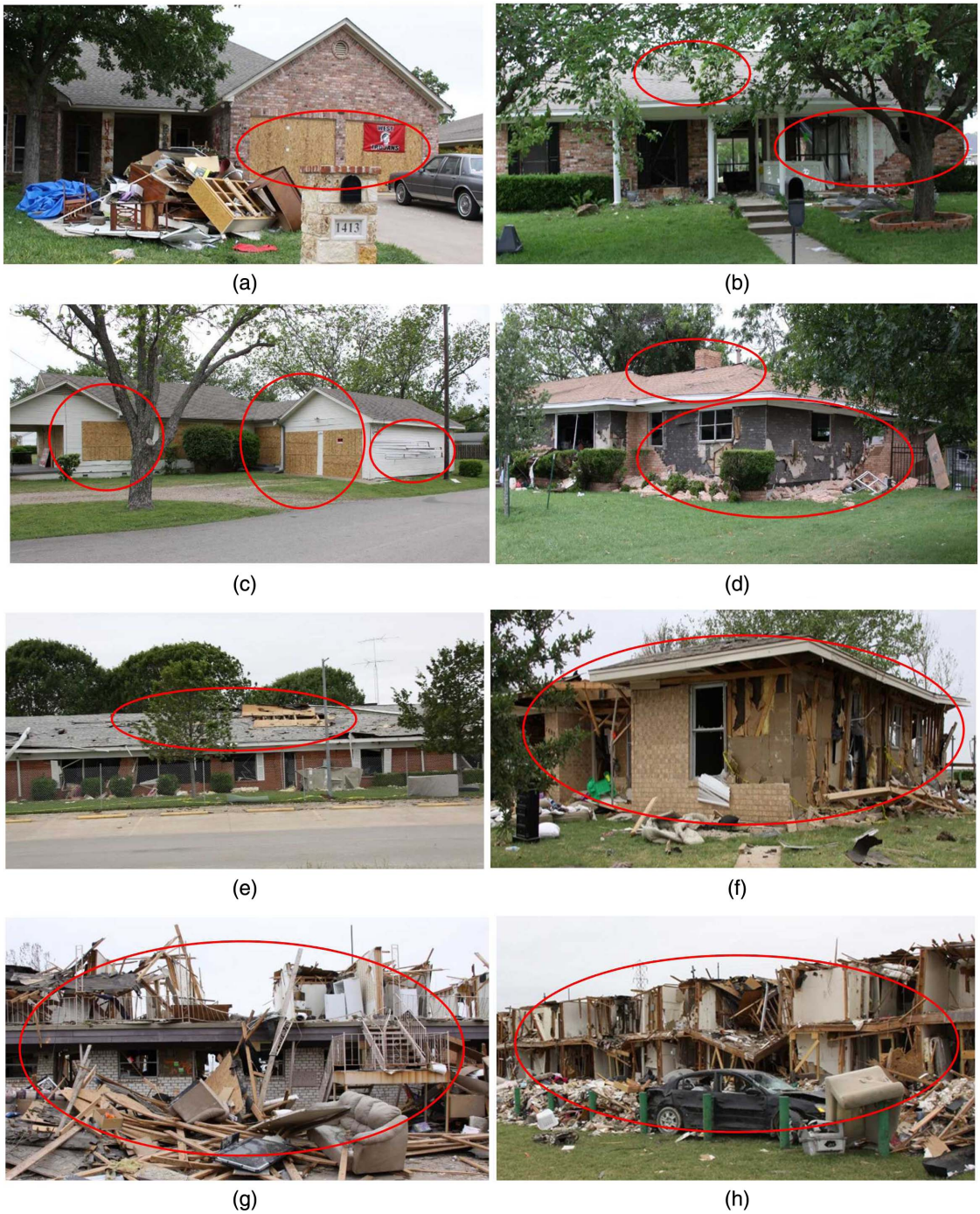

Fig. 1. Damage states DS1 through DS4 in HAZUS Hurricane Model (FEMA 2012) and in Huang et al. (2016): (a) HAZUS Damage state DS1; (b) Huang et al. (2016) Damage state DS1; (c) HAZUS Damage state DS1; (d) Huang et al. (2016) Damage state DS2; (e) HAZUS Damage state DS3; (f) Huang et al. (2016) Damage state DS3; (g) HAZUS Damage state DS4; and (h) Huang et al. (2016) Damage state DS4. (Images by authors.)

incident overpressure (the blast hazard intensity) described in section "Blast Hazard Intensity Measure: Air-Blast Incident Overpressure." Therefore, to better document the data and effectively conduct calculations, an ArcMap geodatabase for the damaged residential buildings for the West fertilizer plant explosion case was created in this study.

ArcMap is a popular tool used to present and edit geospatial information and create digital maps. ArcMap is a component of ArcGIS, which consists of many other applications, such as ArcCatalog, ArcToolbox, ArcScene, ArcGlobe, and ArcGIS Pro. ArcGIS has been used for fragility analysis in previous research. For example, Yao and Xie (2016) evaluated the ecological fragility of a village-township level using the ArcGIS version 9.2 for a mountainous area of southern China, which proposed development strategies for rural spatial restructuring based on landscape security pattern construction as well as a model of rural residential land expansion.

The ArcMap geodatabase created in this study included five important types of data marked on digital maps: (1) geospatial data of the damaged wood light-frame residential buildings for the West fertilizer plant explosion case; (2) geospatial data of the explosion center of the West fertilizer plant explosion; (3) building damage pictures and descriptions inputted as tributary tables for each damaged wood light-frame residential building; (4) damage state information (DS1 through DS4) for each damaged wood light-frame residential building, based on both the HAZUS Hurricane Model and Huang et al. (2016) rating systems; and (5) ArcMap-calculated standoff distances of each damaged building to the explosion center.

Fig. 2(a) demonstrates an ArcMap geodatabase feature class created in this study based on the HAZUS Hurricane Model rating system. Among the 72 damaged wood light-frame residential buildings marked on the map, 0%, 5.5%, 15.5%, and 79.0% were categorized as Damage states DS1 through DS4, respectively. The ArcMap geodatabase feature class shown in Fig. 2(b) was based on the Huang et al. (2016) rating system. It shows that the damaged building counts with Damage states DS1 through DS4 are 45.1%, 29.6%, 18.3%, and 7.0%, respectively.

Empirical Fragility Curve Construction for the West Fertilizer Plant Explosion

Empirical fragility curves were developed for the West fertilizer plant explosion case in this study. The development processes included five key steps: (1) prediction of incident overpressure; (2) damage state classification; (3) determination of damage state frequency distribution; (4) testing for log-normality of fragility relationships; and (5) construction of empirical fragility curves.

Step 1: By assuming TNT-equivalent mass in Section "Blast Hazard Intensity Measure: Air-Blast Incident Overpressure," the air-blast incident overpressure p_s for each of the 72 documented damaged wood residential buildings in the West fertilizer plant explosion was calculated according to both the Held (1983) method and the Unified Facilities Criteria (UFC 2008) method with the standoff distances automatically calculated in the ArcMap geodatabase presented in Fig. 2.

Step 2: The damage state (DS1 through DS4) of each of the 72 documented damaged wood residential buildings in the West fertilizer plant explosion was classified according to Huang et al. (2016) and HAZUS Hurricane Model (FEMA 2012) rating systems as shown in the ArcMap geodatabase in Fig. 2.

Step 3: The frequency distributions of damaged building counts for each damage state (DS1 through DS4) was determined according to Huang et al. (2016) and HAZUS Hurricane Model rating systems. Figs. 3 and 4 show the histograms of the damaged wood residential building counts at different damage states versus the air-blast incident overpressure p_s for the West fertilizer plant explosion case using Huang et al. (2016) and HAZUS Hurricane Model rating systems, respectively. The bin ranges for the p_s in Figs. 3 and 4 are selected based on the theoretical values given in Huang et al. (2016). The bar heights in Figs. 3 and 4 represent the field-investigated number of damaged buildings at each damage state (DS1–DS4). For example, in the p_s range of 6.89–13.79 kPa, theoretically all the building damages should be DS2 (moderate damage) level based on Table 1. However, the field investigation showed that, in this range, three buildings have DS1 damage, 20 have DS2 damage, and six have DS3 damages. This is why the fragility analysis is needed.

As shown in Fig. 4, when the HAZUS Hurricane Model rating system is applied, only three damage states (DS2 through DS4) were obtained and most damaged buildings belonged to DS4 (79% of the total damaged buildings) for the West fertilizer plant explosion case. A distribution with no DS1 and a very high percentage of DS4 may cause problems for goodness-of-fit tests for fragility curves. It was suggested that the damage state rating system for hazardous wind could be ineffective for the blast hazard analysis.

Step 4: The fragility relationships between the blast damage states and the air-blast incident overpressure was proven to be a cumulative lognormal distribution function. The most commonly used probability distribution to describe the posthazard building damage states is the lognormal distribution (FEMA 2012; Jeong and Elnashai 2007; Khalfan et al. 2016). For example, Khalfan et al. (2016) used the cumulative lognormal distribution to describe the fragility relationships between the damage states and PGA for earthquake hazards. HAZUS Hurricane Model (FEMA 2012) used the cumulative lognormal distribution to describe the fragility relationships between the damage states and the wind speed for hurricane hazards. Therefore, this study assumed that the fragility relationships between the blast damage states and the air-blast incident overpressure are a cumulative lognormal distribution function.

The cumulative lognormal distribution function can be written as

$$F_x(D \geq d_j|w_i) = \emptyset\left(\frac{\ln p_i - \mu_i}{\sigma_i}\right) = \frac{1}{2}\left[1 + erf\left(\frac{\ln(p_i) - \mu_i}{\sigma_i\sqrt{2}}\right)\right] \tag{3}$$

where F_x is the probability of a damage state; D is a damage state equal to or greater than the jth damage state, d_j, given an air-blast incident overpressure, p_i; $\emptyset(*)$ = standard normal cumulative distribution function; μ_i and σ_i = logarithmic mean and standard deviation of the jth damage state; erf = Gauss error function; and $erfc$ = complementary error function. There could be associated threshold levels for a given air-blast incident overpressure resulting in separate fragility curves for each damage state.

To validate that the fragility relationship between the blast damage states and the air-blast incident overpressure is a lognormal distribution, the statistics software SPSS Statistics 25 was used to examine the fitness of determined data with the lognormal curve. The Kolmogorov-Smirnov test (KS) (Lilliefors 1969) and the Shapiro-Wilk (SW) test were used to check if the damage data fit lognormal curves. The hypothesis was that the distribution of determined data is not significantly different from a lognormal distribution at a significant level of $\alpha = 0.05$. The test results are presented in Table 2. Because all the KS and SW significance values in Table 2 are greater than $\alpha = 0.05$, except the KS significance value for H-Data 4 using Method 1 for p_s, the hypothesis is accepted. The distributions were validated to be lognormal. The exception of

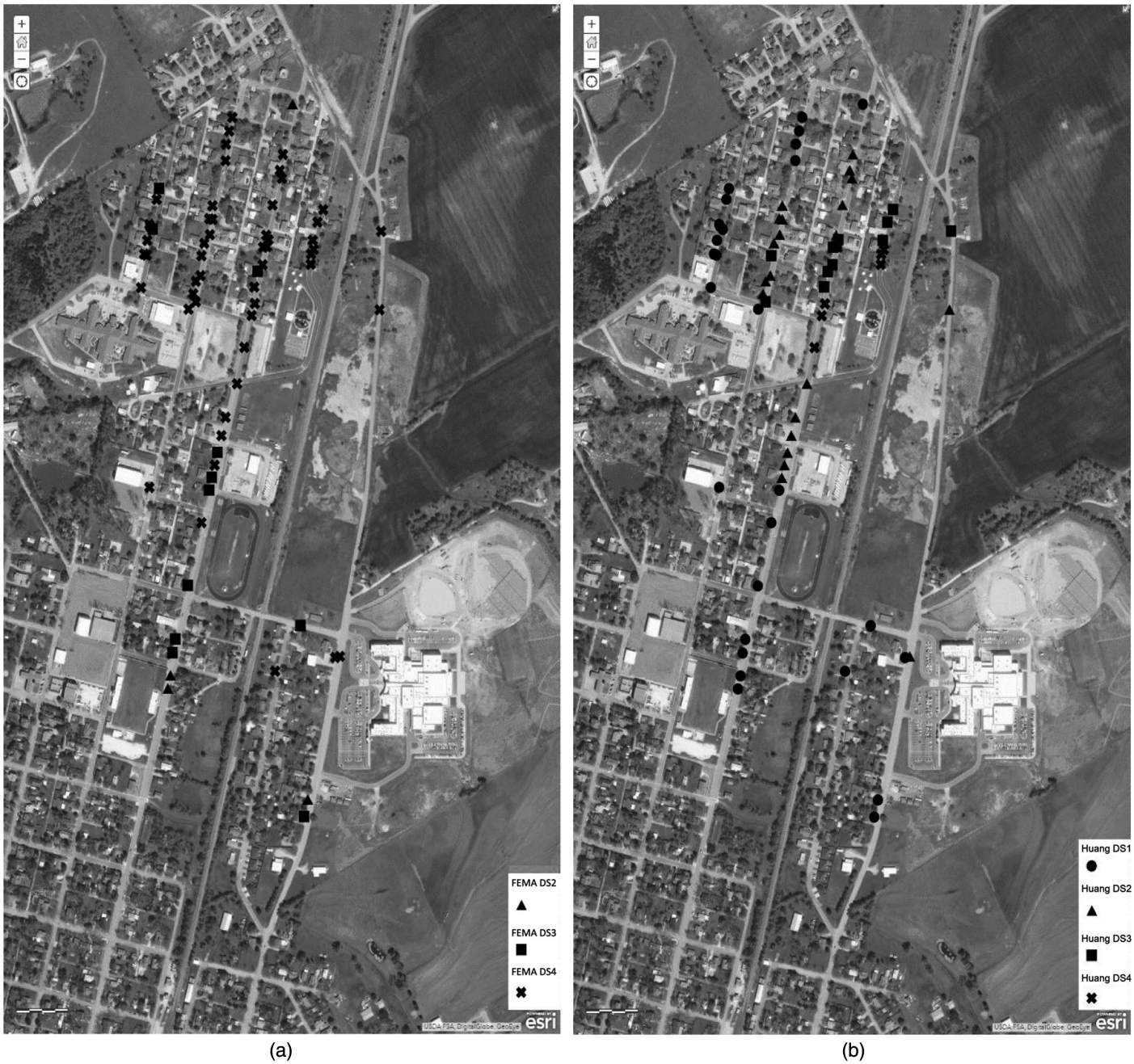

Fig. 2. ArcMap geodatabase for damaged wood light-frame residential buildings for the West fertilizer plant explosion based on (a) HAZUS Hurricane Model; and (b) Huang et al. (2016).

H-Data 4 using Method 1 for p_s may be caused by the small data sample size for that group (only four data values).

Step 5: The empirical fragility curves for the West fertilizer plant explosion case were successfully constructed by the cumulative lognormal distribution function. When performing the cumulative lognormal regression, the probability of each damage state was calculated by dividing the number of buildings being considered. The cumulative probability was then calculated by adding all the probabilities of damage states from the highest damage scale to the damage scale of interest, representing the probability of reaching or exceeding a damage scale at a given air-blast incident overpressure. The cumulative probability values were then fitted with a lognormal fragility function as shown in Eq. (3). A cumulative lognormal curve-fitting program was developed in this study to examine the efficiency and accuracy of the developed curves. The coefficient of determination R^2 was computed.

Figs. 5 and 6 illustrate the resulted fragility curves obtained based on Huang et al. (2016) rating system, as a function of the air-blast incident overpressure p_s. In these figures, the curves marked as H-State 1 through H-State 4 represent the resulted fragility curves for Damage states DS1 through DS4, respectively, and the points marked as H-Data 1 to H-Data 4 represent the field investigated building damage data for Damage states DS1 through DS4, respectively. The "H" designation represented the Huang et al. (2016) rating system. The air-blast incident overpressure p_s was calculated by the Held (1983) method in Fig. 5 and the UFC (2008) method in Fig. 6. As shown in Figs. 5 and 6, Damage state DS1 (minor damage) mostly occurs when the air-blast incident

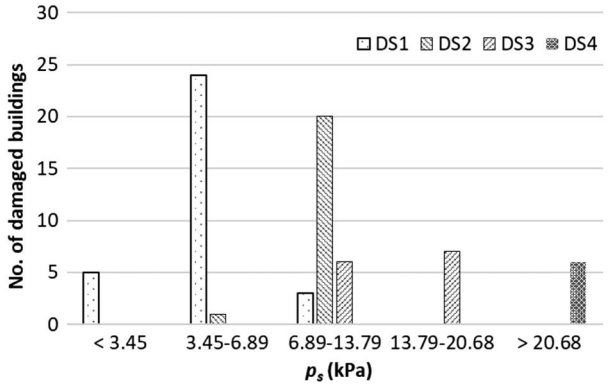

Fig. 3. Damaged building counts histogram according to p_s using the Huang et al. (2016) rating system.

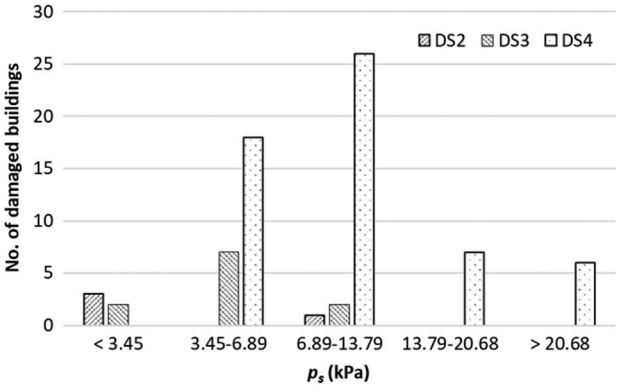

Fig. 4. Damaged building counts histogram according to p_s using the HAZUS Hurricane Model (FEMA 2012) rating system.

overpressure p_s was less than 10 kPa. As the p_s increased, the severity of the building damage increased. Damage state DS2 (moderate damage) mostly occurred when p_s was in the range of 5–15 kPa; the Damage state DS3 (severe damage) mostly occurred when p_s was in the range of 10–20 kPa; and the Damage state DS4 (destructive failure) mostly occurred when p_s was more than 15 kPa. In addition, the shapes and values of the result fragility curves in Figs. 5 and 6 are quite similar for Damage states DS1–DS3. For example, when p_s equals to 10 kPa, Fig. 5 shows that the probabilities of exceedance for DS1 through DS4 are 99%, 73%, 8%, and 0%; and Fig. 6 shows that these probabilities are 96%, 72%, 8%, and 0%. The mean and standard deviation for each curve are presented in Table 2 for comparison. Researchers and users can decide which set of proposed blast fragility curves (Fig. 5 or 6) to use based on their application practice. The Held (1983) p_s calculation method matches the field investigated data better for the West fertilizer plant explosion case. However, the UFC (2008) method is a design provision method, which is more popularly accepted.

Similarly, Figs. 7 and 8 demonstrate the resulted fragility curves expressing the probability of wood residential buildings in this study reaching or exceeding each of the four damage states based on the HAZUS Hurricane Mode (FEMA 2012) rating system, as a function of the air-blast incident overpressure p_s. In these figures, the curves marked as F-State 1 through F-State 4 represent the resulted fragility curves for Damage states DS1 through DS4, respectively, and the points marked as F-Data 1 to F-Data 4 represent the field investigated building damage data for Damage states DS1 through DS4, respectively. The "F" designation represents the FEMA (2012) rating system. The air-blast incident overpressure p_s was calculated by the Held (1983) method in Fig. 7 and the UFC (2008) method in Fig. 8. As shown in Figs. 7 and 8, only three fragility curves, namely, F-State 2, F-State 3 and F-State 4, are shown because no building was classified as Damage state DS1 (minor damage) when using the HAZUS Hurricane Mode (FEMA 2012) rating system. As shown in Figs. 7 and 8, the field investigated damage data was much more scattered than that in Figs. 5 and 6. For example, Damage state DS4 (destruction damage) mostly occurred when the p_s was in the range of 2.6–36 kPa as shown in Fig. 7 and in the range of 4–20 kPa as shown in Fig. 8. The more scattered fragility curves obtained from HAZUS suggest that the Huang et al. damage rating system is more appropriate in case of blast hazard. Therefore, the rating system of Huang et al. (2016) was recommended for the future blast fragility curve construction, and the blast fragility curves in Figs. 5 and 6 are recommended to be used for future prediction of blast fragility.

Table 3 lists the coefficients of determination (R^2) values for the resulted fragility curves developed in this study. As shown in Table 3, all the R^2 values were acceptable (large numbers close to 1) except for one curve (H-Data 4, Method 1). The unacceptable R^2 value (0.487) could be caused by the small sample size for that specific case (only five samples).

Potential users of the proposed blast fragility curves include the following: (1) local government officials, to predict damages of residential buildings in villages, towns, and neighborhoods close to a potential explosion source; (2) local government officials,

Table 2. Significance values of lognormal tests

No.	Sample size	Kolmogorov-Smirnov[a] Method 1 for p_s[b]	Shapiro-Wilk Method 1 for p_s[b]	Kolmogorov-Smirnov[a] Method 2 for p_s[c]	Shapiro-Wilk Method 2 for p_s[c]	Mean	Standard deviation
H-Data 1	32	0.200[d]	0.09	0.164	0.249	3.57	1.29
H-Data 2	21	0.200[d]	0.95	0.200[d]	0.27	8.69	2.30
H-Data 3	13	0.079	0.096	0.200[d]	0.209	15.64	4.03
H-Data 4	5	0.126	0.006	0.200[d]	0.31	29.19	4.11
F-Data 2	4	—	0.206	—	0.761	2.78	2.57
F-Data 3	11	0.200[d]	0.96	0.200[d]	0.777	3.98	2.17
F-Data 4	56	0.200[d]	0.238	0.200[d]	0.092	10.56	7.80

Note: H-Data is the damage state data based on Huang et al. (2016) rating system; F-Data is the damage state data based on HAZUS Hurricane Mode (FEMA 2012) rating system.
[a]Lilliefors significance correction (Lilliefors 1969).
[b]Method 1 for p_s is p_s calculated by the equation in Held (1983).
[c]Method 2 for p_s is p_s calculated by the figure in UFC (2008).
[d]This is a lower bound of the true significance.

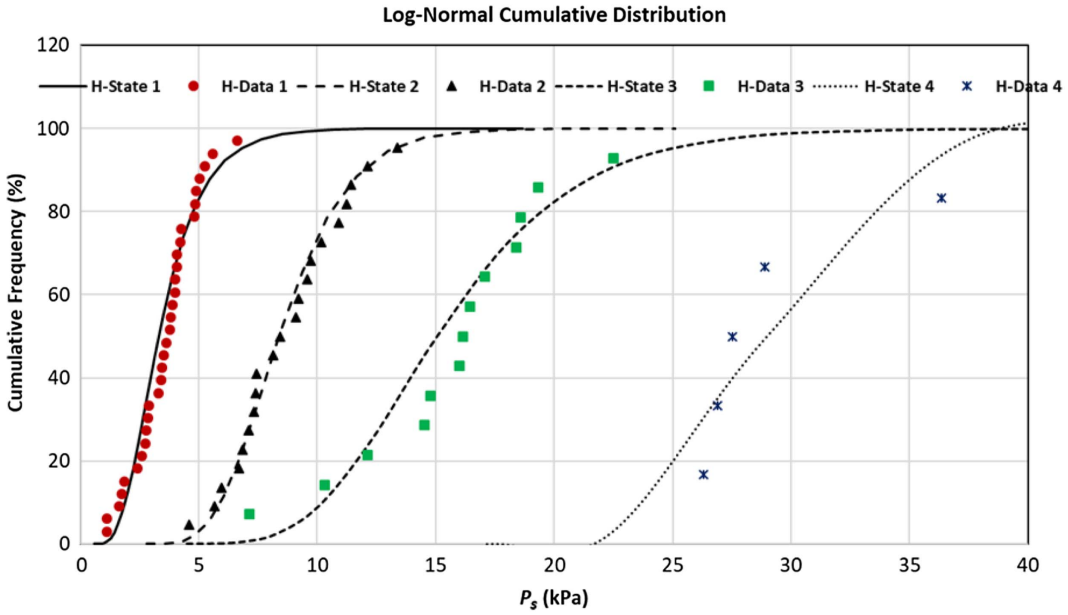

Fig. 5. West fertilizer plant explosion fragility curves of damaged wood residential buildings. Damage states by Huang et al. (2016) and p_s by Held (1983).

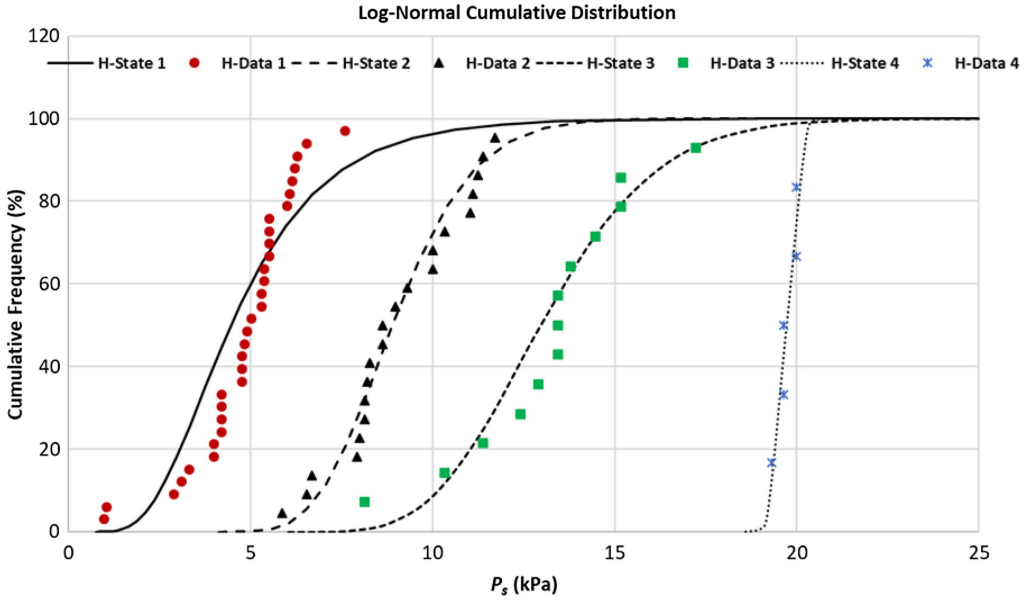

Fig. 6. West fertilizer plant explosion fragility curves of damaged wood residential buildings. Damage states by Huang et al. (2016) and p_s by UFC (2008).

to determine the optimum locations and operational capacities of emergency facilities such as fire stations, emergency centers, and police stations; (3) emergency response teams, to plan and perform emergency response exercises for potential explosions; and (4) federal and state government officials, to estimate total economic losses due to potential explosions, both short- and long-term, to help plan the social, physical, and economic resilience of the communities following explosions.

Conclusion and Future Research

This study developed empirical blast fragility curves for wood residential buildings using the cumulative lognormal distribution function and the real 2013 West fertilizer plant explosion data. A detailed five-step procedure was proposed to help researchers construct empirical blast fragility curves. While classifying the damage states for the fragility curves during the procedure, the Huang et al. (2016) rating system is recommended, while the HAZUS Hurricane model (FEMA 2012) rating system is not recommended for use.

The resultant blast fragility curves of this study can be used to estimate the building damage risks for future explosions and can also provide structural engineers and researchers with fundamental information against blast risks and potential blast design criteria. However, users should keep in mind the limitations of the developed blast fragility curves, which can be only used to estimate losses being considered as an average of a group of similar buildings.

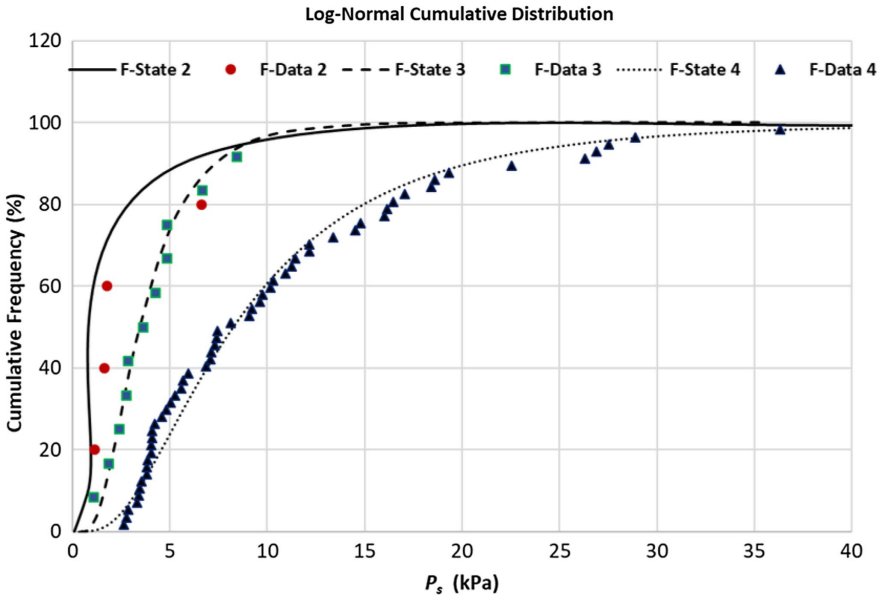

Fig. 7. West fertilizer plant explosion fragility curves of damaged wood residential buildings. Damage state by HAZUS Hurricane Model and p_s by Held (1983).

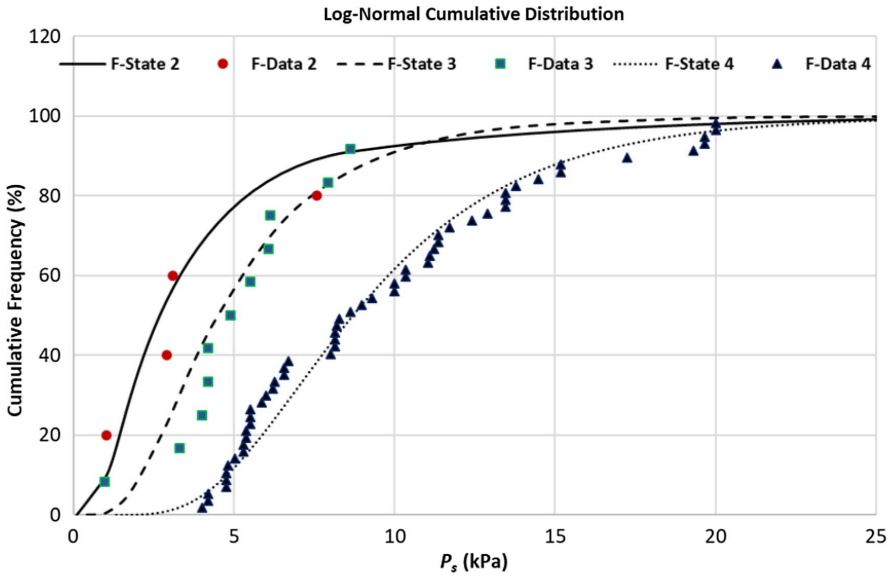

Fig. 8. West fertilizer plant explosion fragility curves of damaged wood residential buildings. Damage state by HAZUS Hurricane Model and p_s by UFC (2008).

Table 3. Correlations of regression results

No.	Sample size	Correlation R^{2a}	Correlation R^{2b}	Notes
H-Data 1	32	0.924	0.836	Using the classification method of Huang et al. (2016)
H-Data 2	21	0.924	0.903	
H-Data 3	13	0.877	0.881	
H-Data 4	5	0.488	0.742	
F-Data 2	4	0.606	0.829	Using classification method of FEMA (2012)
F-Data 3	11	0.960	0.886	
F-Data 4	56	0.9783	0.934	

[a]Regression R^2 based on Method 1, i.e., p_s calculated by the equation in Held (1983).
[b]Regression R^2 based on Method 2, i.e., p_s calculated by the map in UFC (2008).

In many cases, enormously different damages and losses could occur on individual buildings during an explosion.

The blast fragility curve construction is only part of the blast risk assessment procedure. The whole blast risk assessment study for the West fertilizer plant explosion is still considered as a work in progress. Future work may include research and development of more advanced data analytics techniques (e.g., machine learning, deep learning) across heterogeneous, multimedia data. Some of these techniques may only be practical within a virtual information fabric. To explore these issues, the research team is collaborating on the National Science Foundation (NSF)-funded Virtual Information-Fabric Infrastructure (VIFI) for Data-Driven Decisions project (Talukder et al. 2017). Traditional data fabrics require distributed data to be moved to a central location for analysis. When data is

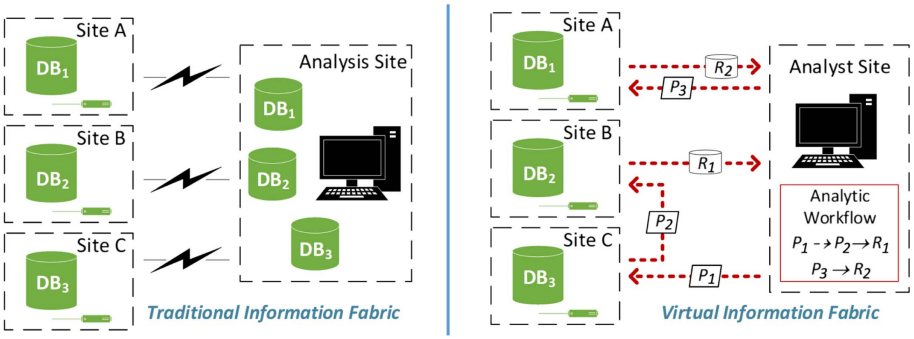

Fig. 9. Traditional information fabrics versus virtual information fabrics.

large, transfer costs can be prohibitive; when data is unshareable, the analysis may be completely unfeasible. Given these challenges, the research team is exploring novel approaches for deploying analytical methods (such as the fragility curve analysis) within what the team described as virtual information fabrics. Within a virtual information fabric (Fig. 9), fragility curve analytics are encapsulated inside reusable, lightweight processing units that can be seamlessly deployed and executed in a distributed fashion. As new data are collected and linked to the virtual information fabric, new analytics can be explored. For example, in the context of this study, the research team conceives of situations that require a more dynamic application of fragility curves as new structures are constructed, existing structures are modified, and spatial properties change. Moreover, the team sees the potential benefits of integrating fragility curves with additional data and analytics to provide better assessments to structural engineers, architects, urban planners, first responders, and policy makers.

Data Availability Statement

Some data, models, or code generated or used during the study are available from the corresponding author by request, such as building damage pictures, ArcGIS geodatabase, and the fragility analysis document.

Acknowledgments

This paper is based on work supported by the National Science Foundation under Grant No. ACI-1640818. Any opinions, findings, and conclusions or recommendations expressed in this paper are those of the authors and do not necessarily reflect the views of the National Science Foundation.

References

Abdollahzadeh, G., and M. Nemati. 2014. "Risk assessment of structures subjected to blast." *Int. J. Damage Mech.* 23 (1): 3–24. https://doi.org/10.1177/1056789513482479.

Ataei, N., and J. E. Padgett. 2015. "Fragility surrogate models for coastal bridges in hurricane-prone zones." *Eng. Struct.* 103 (2015): 203–213. https://doi.org/10.1016/j.engstruct.2015.07.002.

Babrauskas, V. 2016. "Explosions of ammonium nitrate fertilizer in storage or transportation are preventable accidents." *J. Hazard. Mater.* 304 (Mar): 134–149. https://doi.org/10.1016/j.jhazmat.2015.10.040.

Babrauskas, V. 2017. "The West, Texas, ammonium nitrate explosion: A failure of regulation." *J. Fire Sci.* 35 (5): 396–414. https://doi.org/10.1177/0734904116685723.

Baker, W. E., P. A. Cox, P. S. Westine, J. J. Kulesz, and R. A. Strehlow. 1983. *Explosion hazards and evaluation*. New York: Elsevier.

Brode, H. L. 1955. "Numerical solution of spherical blast waves." *J. Appl. Phys.* 26 (6): 766–775. https://doi.org/10.1063/1.1722085.

Calabresea, A., and C. G. Lai. 2013. "Fragility functions of blockwork wharves using artificial neural networks." *Soil Dyn. Earthquake Eng.* 52 (Sept): 88–102. https://doi.org/10.1016/j.soildyn.2013.05.002.

Chang, D. B., and C. S. Young. 2010. "Probabilistic estimates of vulnerability to explosive overpressures and impulses." *J. Phys. Secur.* 4 (2): 10–29. https://doi.org/10.1.1.648.4991.

Dai, K., J. Wang, Z. Huang, and H. F. Wu. 2016. "Investigations of structural damage caused by the fertilizer plant explosion at West, Texas. II: Ground shock." *J. Perform. Constr. Facil.* 30 (4): 04015065. https://doi.org/10.1061/(ASCE)CF.1943-5509.0000800.

Davis, S., T. DeBold, and C. Marsegan. 2017. "Investigation findings and lessons learned in the west fertilizer explosion." *J. Fire Sci.* 35 (5): 379–395. https://doi.org/10.1177/0734904117715649.

Faghihmaleki, H., F. Nejati, A. Mirzagoltabar-Roshan, and Y. Batebi-Motlagh. 2017. "An evaluation of multi-hazard risk subjected to blast and earthquake loads in RC moment frame with shear wall." *J. Eng. Sci. Technol.* 12 (3): 636–647. https://doi.org/10.1061/(ASCE)CF.1943-5509.0001016.

FEMA. 2009. *Multi-hazard loss estimation methodology-hurricane model: HAZUS-MH-MR4 technical manual*. Washington, DC: FEMA.

FEMA. 2011. *Hazards U.S. multi-hazard (HAZUS MH) assessment tool.* Vol.3. Washington, DC: FEMA.

FEMA. 2012. *Multi-hazard loss estimation methodology-Hurricane model: HAZUS-MH 2.1 Technical manual*. Washington, DC: FEMA.

Fulvio, P. 2015. "Blast fragility and performance-based pressure–impulse diagrams of European reinforced concrete columns." *Eng. Struct.* 103 (Nov): 285–297. https://doi.org/10.1016/j.engstruct.2015.09.019.

Gernay, T., N. Elhami Khorasani, and M. Garlock. 2016. "Fire fragility curves for steel buildings in a community context: A methodology." *Eng. Struct.* 113 (Apr): 259–276. https://doi.org/10.1016/j.engstruct.2016.01.043.

Ghosh, J., J. E. Padgett, and L. Dueas-Osorio. 2013. "Surrogate modeling and failure surface visualization for efficient seismic vulnerability assessment of highway bridges." *Probab. Eng. Mech.* 34 (Oct): 189–199. https://doi.org/10.1016/j.probengmech.2013.09.003.

Han, Z., H. J. Pasman, and M. S. Mannan. 2017. "Extinguishing fires involving ammonium nitrate stock with water: Possible complications." *J. Fire Sci.* 35 (6): 457–483. https://doi.org/10.1177/0734904117735264.

Han, Z., S. Sachdeva, M. I. Papadaki, and S. Mannan. 2016. "Effects of inhibitor and promoter mixtures on ammonium nitrate fertilizer explosion hazards." *Thermochimica Acta* 624 (Jan): 69–75. https://doi.org/10.1016/j.tca.2015.12.005.

Held, M. 1983. "Blast waves in free air." *Propellants, Explos. Pyrotech.* 8 (1): 1–7. https://doi.org/10.1002/prep.19830080102.

Henrych, J. 1979. *The dynamics of explosion and its use*. Amsterdam, Netherlands: Elsevier.

Herbin, A. H., and M. Barbato. 2012. "Fragility curves for building envelope components subject to windborne debris impact." *J. Wind*

Eng. Ind. Aerodyn. 107–108 (Aug): 285–298. https://doi.org/10.1016/j.jweia.2012.05.005.

Huang, Z., K. Dai, J. Wang, and H. F. Wu. 2016. "Investigations of structural damage caused by the fertilizer plant explosion at West, Texas. I: Air-blast incident overpressure." *J. Perform. Constr. Facil.* 30 (4): 04015064. https://doi.org/10.1061/(ASCE)CF.1943-5509.0000799.

Jennings, K., and C. Matthiessen. 2015. "Update: EPA actions-chemical safety and security executive order." *Process Saf. Prog.* 34 (2): 196–198. https://doi.org/10.1002/prs.11707.

Jeong, S. H., and A. S. Elnashai. 2007. "Probabilistic fragility analysis parameterized by fundamental response quantities." *Eng. Struct.* 29 (6): 1238–1251. https://doi.org/10.1016/j.engstruct.2006.06.026.

Khalfan, M., W. W. El-Dakhakhni, and M. J. Tait. 2016. "Seismic risk assessment of nonengineered residential buildings in developing countries." *J. Perform. Constr. Facil.* 30 (5): 04016013. https://doi.org/10.1061/(ASCE)CF.1943-5509.0000829.

Konthesingha, C., M. G. Stewart, P. C. Ryan, J. D. Ginger, and D. J. Henderson. 2015. "Reliability-based vulnerability modeling of metal-clad industrial buildings to extreme wind loading for cyclonic regions." *J. Wind Eng. Ind. Aerodyn.* 147 (Dec): 176–185. https://doi.org/10.1016/j.jweia.2015.10.002.

Kunnath, S. K. 2018. "Modeling of reinforced concrete structures for nonlinear seismic simulation." *J. Struct. Integrity Maint.* 3 (3): 137–149. https://doi.org/10.1080/24705314.2018.1492669.

Laboureur, D. M., Z. Han, B. Z. Harding, A. Pineda, William C. Pittman, C. Rosas, J. Jiang, and M. S. Mannan. 2016. "Case study and lessons learned from the ammonium nitrate explosion at the West fertilizer facility." *J. Hazard. Mater.* 308 (May): 164–172. https://doi.org/10.1016/j.jhazmat.2016.01.039.

Lagaros, N. D., and M. Fragiadakis. 2007. "Fragility assessment of steel frames using neural networks." *Earthquake Spectra* 23 (4): 735–752. https://doi.org/10.1193/1.2798241.

Lallemant, D., A. Kiremidjian, and H. Burton. 2015. "Statistical procedures for developing earthquake damage fragility curves." *Earthquake Eng. Struct. Dyn.* 44 (9): 1373–1389. https://doi.org/10.1002/eqe.2522.

Lilliefors, H. 1969. "On the Kolmogorov–Smirnov test for the exponential distribution with mean unknown." *J. Am. Stat. Assoc.* 64 (325): 387–389. https://doi.org/10.1080/01621459.1969.10500983.

Macabuag, J., T. Rossetto, I. Ioannou, and I. EamesI. 2018. "Investigation of the effect of debris-induced damage for constructing tsunami fragility curves for buildings." *Geosciences* 8 (4): 117. https://doi.org/10.3390/geosciences8040117.

Mai, C., K. Konakli, and B. Sudret. 2017. "Seismic fragility curves for structures using non-parametric representations." *Front. Struct. Civ. Eng.* 11 (2): 169–186. https://doi.org/10.1007/s11709-017-0385-y.

Maloney, T., B. Ellingwood, H. Mahmoud, N. Wang, Y. Wang, and P. Lin. 2018. "Performance and risk to light-framed wood residential buildings subjected to tornadoes." *Struct. Saf.* 70 (Jan): 35–47. https://doi.org/10.1016/j.strusafe.2017.10.004.

Mills, C. A. 1987. "The design of the concrete structure to resist explosions and weapon effects." In *Proc., 1st Int. Conf. on Concrete for Hazard Protections*, 61–73. Lausanne, Switzerland: International Federation for Structural Concrete.

Mishra, S., O. A. Vanli, B. P. Alduse, and S. Jung. 2017. "Hurricane loss estimation in wood-frame buildings using Bayesian model updating: Assessing uncertainty in fragility and reliability analyses." *Eng. Struct.* 135 (Mar): 81–94. https://doi.org/10.1016/j.engstruct.2016.12.063.

Mitropoulou, C. C., and M. Papadrakakis. 2011. "Developing fragility curves based on neural network IDA predictions." *Eng. Struct.* 33 (12): 3409–3421. https://doi.org/10.1016/j.engstruct.2011.07.005.

Noh, H. Y., D. Lallemant, and A. S. Kiremidjian. 2015. "Development of empirical and analytical fragility functions using kernel smoothing methods." *Earthquake Eng. Struct. Dyn.* 44 (8): 1163–1180. https://doi.org/10.1002/eqe.2505.

Rehman, K., and Y. S. Cho. 2018. "Building damage assessment using scenario-based tsunami numerical analysis and fragility curves." *Water* 8 (3): 109–126. https://doi.org/10.3390/w8030109.

Rossetto, T., and A. S. Elnashai. 2003. "Derivation of vulnerability functions for European-type RC structures based on observational data." *Eng. Struct.* 25 (10): 1241–1263. https://doi.org/10.1016/S0141-0296(03)00060-9.

Shinozuka, M., M. Q. Feng, J. Lee, and T. Naganuma. 2000. "Statistical analysis of fragility curves." *J. Eng. Mech.* 126 (12): 1224–1231. https://doi.org/10.1061/(ASCE)0733-9399(2000)126:12(1224).

Stewart, M. G., and M. D. Netherton. 2008. "Security risks and probabilistic risk assessment of glazing subject to explosive blast loading." *Reliab. Eng. Syst. Saf.* 93 (4): 627–638. https://doi.org/10.1016/j.ress.2007.03.007.

Stewart, M. G., P. C. Ryan, D. J. Henderson, and J. D. Ginger. 2016. "Fragility analysis of roof damage to industrial buildings subject to extreme wind loading in non-cyclonic regions." *Eng. Struct.* 128 (Dec): 333–343. https://doi.org/10.1016/j.engstruct.2016.09.053.

Talukder, A., M. Elshambakey, S. Wadkar, H. Lee, L. Cinquini, S. Schlueter, I. Cho, W. Dou, and D. J. Crichton. 2017. "VIFI: Virtual information fabric infrastructure for data-driven discoveries from distributed earth science data." In *Proc., 2017 IEEE SmartWorld, Ubiquitous Intelligence & Computing, Advanced & Trusted Computed, Scalable Computing & Communications, Cloud & Big Data Computing, Internet of People and Smart City Innovation (SmartWorld/SCALCOM/UIC/ATC/CBDCom/IOP/SCI)*, 1–8, New York: IEEE.

UFC (Unified Facilities Criteria). 2008. "*Structures to resist the effects of accidental explosions.*" UFC 3-340-02. Las Vegas: UFC.

Veneziano, D., F. Casciati, and L. Faravelli. 1983. "Method of seismic fragility for complicated systems." In *Probabilistic methods in seismic risk assessment for nuclear power plants*. Cambridge, MA: MIT Press.

Wang, Z., N. Pedroni, I. Zentner, and E. Zioc. 2018. "Seismic fragility analysis with artificial neural networks: Application to nuclear power plant equipment." *Eng. Struct.* 162 (May): 213–225. https://doi.org/10.1016/j.engstruct.2018.02.024.

Yao, G., and H. Xie. 2016. "Rural spatial restructuring in ecologically fragile mountainous areas of southern China: A case study of Changgang town, Jiangxi province." *J. Rural Stud.* 47 (Oct): 435–448. https://doi.org/10.1016/j.jrurstud.2016.07.014.

Yonekawa, Y., et al. 2014. "Ocular blast injuries in mass-casualty incidents the marathon bombing in Boston, Massachusetts, and the fertilizer plant explosion in West, Texas." *Ophthalmology* 121 (9): 1670–1676. https://doi.org/10.1016/j.ophtha.2014.04.004.

Yu, R., L. Chen, Q. Fang, and Y. Huan. 2018. "An improved nonlinear analytical approach to generate fragility curves of reinforced concrete columns subjected to blast loads." *Adv. Struct. Eng.* 21 (3): 396–414. https://doi.org/10.1177/1369433217718986.

Zentner, I., M. Gündel, and N. Bonfils. 2017. "Fragility analysis methods: A review of existing approaches and application." *Nucl. Eng. Des.* 323 (Nov): 245–258. https://doi.org/10.1016/j.nucengdes.2016.12.021.